Julius-Maximilians-
UNIVERSITÄT
WÜRZBURG

NLO QCD predictions for polarised W^+Z production with semileptonic decay

Christoph Haitz
in collaboration with Ansgar Denner and Giovanni Pelliccioli

Institut für Theoretische Physik 2
Julius-Maximilians-Universität Würzburg

08.03.2023

based on arXiv:2211.09040 (accepted by PRD)

Table of contents

Motivation

- Polarised processes allow for deep insights into spontaneous symmetry breaking
- Polarised cross-sections are very sensitive to beyond-Standard Model effects
- Polarisation is well suited for tests of the Standard Model
- Polarised WZ production processes are a subject of ongoing research

Existing Work on polarised ZW production

- Focus is on purely leptonic decay modes
- Narrow-width approximation
  - MadGraph5_aMC@NLO LO-study, Buarque Franzosi et al. 2020, arXiv:1912.01725 [1]
- Double-pole approximation
  - NLO QCD, Denner and Pellicciolo 2021, arXiv:2010.07149 [2]
  - NLO QCD und NLO EW, Le and Baglio 2022, arXiv:2203.01470 [3], Le et al. 2022, arXiv:2208.09232 [4], Le et al. 2022, arXiv:2302.03324 [5]
- Experimental studies
  - ATLAS 2019, arXiv:1902.05759 [6]
  - CMS 2022, arXiv:2110.11231 [7]
  - ATLAS 2022, arXiv:2211.09435 [8] (next talk)

Definition of polarised cross-sections

- Diagrams with and without the wanted (s-channel) resonance contribute to a given process

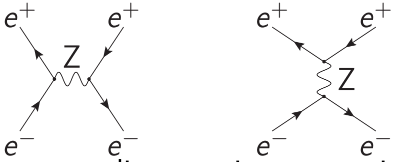

- Remove non-resonant diagrams in a gauge-independent way
  - This can be achieved by using a pole approximation
    - ⋆ Set resonant particles on-shell $\{p_i\} \Rightarrow \{\tilde{p}_i\}$
    - ⋆ Conserve some off-shell effects by using the off-shell denominators of the propagators and applying the phase-space cuts to the off-shell momenta

$$M\left(\{\tilde{p}\}, p_{res}^2\right) = M_{\mu,\text{production}}\left(\{\tilde{p}\}\right) \frac{N^{\mu\nu}\left(\{\tilde{p}\}\right)}{p_{res}^2 - m^2 - im\Gamma} M_{\nu,\text{decay}}\left(\{\tilde{p}\}\right)$$

Definition of polarised cross-sections

- Numerator of the resonant propagator contains a sum over all polarisation states

$$\sum_{\text{polarisations}} \epsilon^*_\mu \epsilon_\nu = -g_{\mu\nu} \quad \text{(Feynman-´t Hooft gauge)}$$

$$M\left(\{\tilde{p}\}, p^2_{res}\right) = \sum_\lambda M_{\mu,\text{production}}\left(\{\tilde{p}\}\right) \frac{\epsilon^{\mu*}_\lambda\left(\{\tilde{p}\}\right)\epsilon^\nu_\lambda\left(\{\tilde{p}\}\right)}{p^2_{res} - m^2 - im\Gamma} M_{\nu,\text{decay}}\left(\{\tilde{p}\}\right)$$

$$M\left(\{\tilde{p}\}, p^2_{res}\right) = \sum_\lambda M_\lambda\left(\{\tilde{p}\}, p^2_{res}\right)$$

Definition of polarised cross-sections

- Take the square of the matrix element to calculate the cross-section

$$\underbrace{\left|M\left(\{\tilde{p}\}, p_{res}^2\right)\right|^2}_{\text{unpolarised}} = \sum_{\lambda} \underbrace{\left|M_\lambda\left(\{\tilde{p}\}, p_{res}^2\right)\right|^2}_{\text{polarisation } \lambda} + \underbrace{\sum_{\lambda \neq \lambda'} M_\lambda^*\left(\{\tilde{p}\}, p_{res}^2\right) M_{\lambda'}\left(\{\tilde{p}\}, p_{res}^2\right)}_{\text{interferences}}$$

Setup

$$p\,p \to Z(\to e^- e^+)\,W^+(\to jets)$$

- Z boson decays leptonically into an electron-positron pair
- W^+ boson decays hadronically (jet system)
- Polarisation is defined in the center-of-mass frame of the two bosons
- Resolved setup
  - Two light jets (AK4)
  - Jet system = the two jets with an invariant mass closest to the W-mass
- Unresolved setup
  - One massive fat jet (AK8)
  - Jet system = fat jet with the largest transverse momentum

Phase-space cuts

- Phase-space cuts mimic the CMS analysis arXiv:2111.13669 [9]
- Different phase-space cuts are applied in the two setups
- Suppress non-resonant background
- Z and W^+ are very boosted
- Anti-kT jet algorithm
  - Resolved: $R_0 = 0.4$
  - Unresolved: $R_0 = 0.8$

		resolved	unresolved
Jet selection	min p_T	30 GeV	200 GeV
	max $\|y\|$	2.4	2.4
	min $\Delta R_{Jl^\pm}$	0.4	0.8
	min M	-	65 GeV
	max M	-	105 GeV
Cuts on the jet system (W^+-Boson)	min p_T	200 GeV	-
	min M	65 GeV	-
	max M	105 GeV	-
Cuts on single leptons	min p_T	40 GeV	40 GeV
	max $\|y\|$	2.4	2.4
Cuts on the lepton pair (Z-Boson)	min p_T	200 GeV	200 GeV
	min M	76 GeV	76 GeV
	max M	106 GeV	106 GeV

Integrated results

state	σ_{LO} [fb]	f_{LO}[%]	σ_{NLO} [fb]	f_{NLO}[%]	K_{NLO}	$K_{\mathrm{NLO}}^{(\mathrm{no\ g})}$
resolved, $Z(e^+e^-)W^+(jj)$						
unpol.	$1.8567(2)^{+1.2\%}_{-1.4\%}$	100	$3.036(2)^{+6.8\%}_{-5.3\%}$	100	1.635	1.033
$Z_L W_L^+$	$0.64603(5)^{+0.2\%}_{-0.6\%}$	34.8	$0.6127(4)^{+0.9\%}_{-0.7\%}$	20.2	0.948	1.031
$Z_L W_T^+$	$0.08687(1)^{+0.2\%}_{-0.6\%}$	4.7	$0.17012(6)^{+8.6\%}_{-6.8\%}$	5.6	1.958	0.967
$Z_T W_L^+$	$0.08710(1)^{+0.1\%}_{-0.6\%}$	4.7	$0.24307(7)^{+10.2\%}_{-8.2\%}$	8.0	2.791	1.017
$Z_T W_T^+$	$0.97678(7)^{+2.0\%}_{-2.2\%}$	52.6	$2.0008(7)^{+8.9\%}_{-7.1\%}$	65.8	2.048	1.059
interf.	0.0595(1)	3.2	0.009(2)	0.4	–	–
unresolved, $Z(e^+e^-)W^+(J)$						
unpol.	$1.6879(2)^{+1.9\%}_{-2.1\%}$	100	$3.112(2)^{+7.6\%}_{-6.1\%}$	100	1.843	1.193
$Z_L W_L^+$	$0.61653(5)^{+1.0\%}_{-1.3\%}$	36.5	$0.6799(5)^{+0.9\%}_{-0.7\%}$	21.9	1.103	1.170
$Z_L W_T^+$	$0.06444(1)^{+0.7\%}_{-1.0\%}$	3.8	$0.17584(6)^{+10.8\%}_{-8.6\%}$	5.7	2.729	1.158
$Z_T W_L^+$	$0.07437(1)^{+0.6\%}_{-0.9\%}$	4.4	$0.24742(8)^{+11.0\%}_{-8.9\%}$	8.0	3.327	1.193
$Z_T W_T^+$	$0.88233(9)^{+2.9\%}_{-2.9\%}$	52.3	$2.0041(8)^{+9.6\%}_{-7.7\%}$	64.3	2.271	1.227
interf.	0.0503(3)	3.0	0.004(2)	0.1	–	–

Integrated results

state	σ_{LO} [fb]	f_{LO}[%]	σ_{NLO} [fb]	f_{NLO}[%]	K_{NLO}	$K_{\mathrm{NLO}}^{(\mathrm{no\ g})}$
resolved, $Z(e^+e^-)W^+(jj)$						
unpol.	$1.8567(2)^{+1.2\%}_{-1.4\%}$	100	$3.036(2)^{+6.8\%}_{-5.3\%}$	100	1.635	1.033
$Z_L W_L^+$	$0.64603(5)^{+0.2\%}_{-0.6\%}$	34.8	$0.6127(4)^{+0.9\%}_{-0.7\%}$	20.2	0.948	1.031
$Z_L W_T^+$	$0.08687(1)^{+0.2\%}_{-0.6\%}$	4.7	$0.17012(6)^{+8.6\%}_{-6.8\%}$	5.6	1.958	0.967
$Z_T W_L^+$	$0.08710(1)^{+0.1\%}_{-0.6\%}$	4.7	$0.24307(7)^{+10.2\%}_{-8.2\%}$	8.0	2.791	1.017
$Z_T W_T^+$	$0.97678(7)^{+2.0\%}_{-2.2\%}$	52.6	$2.0008(7)^{+8.9\%}_{-7.1\%}$	65.8	2.048	1.059
interf.	0.0595(1)	3.2	0.009(2)	0.4	—	—
unresolved, $Z(e^+e^-)W^+(J)$						
unpol.	$1.6879(2)^{+1.9\%}_{-2.1\%}$	100	$3.112(2)^{+7.6\%}_{-6.1\%}$	100	1.843	1.193
$Z_L W_L^+$	$0.61653(5)^{+1.0\%}_{-1.3\%}$	36.5	$0.6799(5)^{+0.9\%}_{-0.7\%}$	21.9	1.103	1.170
$Z_L W_T^+$	$0.06444(1)^{+0.7\%}_{-1.0\%}$	3.8	$0.17584(6)^{+10.8\%}_{-8.6\%}$	5.7	2.729	1.158
$Z_T W_L^+$	$0.07437(1)^{+0.6\%}_{-0.9\%}$	4.4	$0.24742(8)^{+11.0\%}_{-8.9\%}$	8.0	3.327	1.193
$Z_T W_T^+$	$0.88233(9)^{+2.9\%}_{-2.9\%}$	52.3	$2.0041(8)^{+9.6\%}_{-7.7\%}$	64.3	2.271	1.227
interf.	0.0503(3)	3.0	0.004(2)	0.1	—	—

- Large NLO corrections mostly from gluon initiated real emission processes

Integrated results

state	$\sigma_{\rm LO}$ [fb]	$f_{\rm LO}$[%]	$\sigma_{\rm NLO}$ [fb]	$f_{\rm NLO}$[%]	$K_{\rm NLO}$	$K_{\rm NLO}^{(\rm no\ g)}$
resolved, $Z(e^+e^-)W^+(jj)$						
unpol.	$1.8567(2)^{+1.2\%}_{-1.4\%}$	100	$3.036(2)^{+6.8\%}_{-5.3\%}$	100	1.635	1.033
$Z_L W^+_L$	$0.64603(5)^{+0.2\%}_{-0.6\%}$	34.8	$0.6127(4)^{+0.9\%}_{-0.7\%}$	20.2	0.948	1.031
$Z_L W^+_T$	$0.08687(1)^{+0.2\%}_{-0.6\%}$	4.7	$0.17012(6)^{+8.6\%}_{-6.8\%}$	5.6	1.958	0.967
$Z_T W^+_L$	$0.08710(1)^{+0.1\%}_{-0.6\%}$	4.7	$0.24307(7)^{+10.2\%}_{-8.2\%}$	8.0	2.791	1.017
$Z_T W^+_T$	$0.97678(7)^{+2.0\%}_{-2.2\%}$	52.6	$2.0008(7)^{+8.9\%}_{-7.1\%}$	65.8	2.048	1.059
interf.	0.0595(1)	3.2	0.009(2)	0.4	–	–
unresolved, $Z(e^+e^-)W^+(J)$						
unpol.	$1.6879(2)^{+1.9\%}_{-2.1\%}$	100	$3.112(2)^{+7.6\%}_{-6.1\%}$	100	1.843	1.193
$Z_L W^+_L$	$0.61653(5)^{+1.0\%}_{-1.3\%}$	36.5	$0.6799(5)^{+0.9\%}_{-0.7\%}$	21.9	1.103	1.170
$Z_L W^+_T$	$0.06444(1)^{+0.7\%}_{-1.0\%}$	3.8	$0.17584(6)^{+10.8\%}_{-8.6\%}$	5.7	2.729	1.158
$Z_T W^+_L$	$0.07437(1)^{+0.6\%}_{-0.9\%}$	4.4	$0.24742(8)^{+11.0\%}_{-8.9\%}$	8.0	3.327	1.193
$Z_T W^+_T$	$0.88233(9)^{+2.9\%}_{-2.9\%}$	52.3	$2.0041(8)^{+9.6\%}_{-7.7\%}$	64.3	2.271	1.227
interf.	0.0503(3)	3.0	0.004(2)	0.1	–	–

- Large contribution of the purely longitudinal polarisation state compared to more inclusive set-ups (no strong p_T cut) [2]
- Goldstone boson contributions are unsuppressed because diagrams with three gauge-boson vertices contribute at LO

Integrated results

state	σ_{LO} [fb]	f_{LO}[%]	σ_{NLO} [fb]	f_{NLO}[%]	K_{NLO}	$K_{\mathrm{NLO}}^{(\mathrm{no\ g})}$
resolved, $Z(e^+e^-)W^+(jj)$						
unpol.	$1.8567(2)^{+1.2\%}_{-1.4\%}$	100	$3.036(2)^{+6.8\%}_{-5.3\%}$	100	1.635	1.033
$Z_L W_L^+$	$0.64603(5)^{+0.2\%}_{-0.6\%}$	34.8	$0.6127(4)^{+0.9\%}_{-0.7\%}$	20.2	0.948	1.031
$Z_L W_T^+$	$0.08687(1)^{+0.2\%}_{-0.6\%}$	4.7	$0.17012(6)^{+8.6\%}_{-6.8\%}$	5.6	1.958	0.967
$Z_T W_L^+$	$0.08710(1)^{+0.1\%}_{-0.6\%}$	4.7	$0.24307(7)^{+10.2\%}_{-8.2\%}$	8.0	2.791	1.017
$Z_T W_T^+$	$0.97678(7)^{+2.0\%}_{-2.2\%}$	52.6	$2.0008(7)^{+8.9\%}_{-7.1\%}$	65.8	2.048	1.059
interf.	0.0595(1)	3.2	0.009(2)	0.4	—	—
unresolved, $Z(e^+e^-)W^+(J)$						
unpol.	$1.6879(2)^{+1.9\%}_{-2.1\%}$	100	$3.112(2)^{+7.6\%}_{-6.1\%}$	100	1.843	1.193
$Z_L W_L^+$	$0.61653(5)^{+1.0\%}_{-1.3\%}$	36.5	$0.6799(5)^{+0.9\%}_{-0.7\%}$	21.9	1.103	1.170
$Z_L W_T^+$	$0.06444(1)^{+0.7\%}_{-1.0\%}$	3.8	$0.17584(6)^{+10.8\%}_{-8.6\%}$	5.7	2.729	1.158
$Z_T W_L^+$	$0.07437(1)^{+0.6\%}_{-0.9\%}$	4.4	$0.24742(8)^{+11.0\%}_{-8.9\%}$	8.0	3.327	1.193
$Z_T W_T^+$	$0.88233(9)^{+2.9\%}_{-2.9\%}$	52.3	$2.0041(8)^{+9.6\%}_{-7.7\%}$	64.3	2.271	1.227
interf.	0.0503(3)	3.0	0.004(2)	0.1	—	—

- Significant differences between the resolved and unresolved setup at LO caused by the recombination of the jets
- Differences become smaller at NLO

Integrated results

state	$\sigma_{\rm LO}$ [fb]	$f_{\rm LO}$[%]	$\sigma_{\rm NLO}$ [fb]	$f_{\rm NLO}$[%]	$K_{\rm NLO}$	$K_{\rm NLO}^{\rm (no\ g)}$
resolved, $Z(e^+e^-)W^+(jj)$						
unpol.	$1.8567(2)^{+1.2\%}_{-1.4\%}$	100	$3.036(2)^{+6.8\%}_{-5.3\%}$	100	1.635	1.033
$Z_L W_L^+$	$0.64603(5)^{+0.2\%}_{-0.6\%}$	34.8	$0.6127(4)^{+0.9\%}_{-0.7\%}$	20.2	0.948	1.031
$Z_L W_T^+$	$0.08687(1)^{+0.2\%}_{-0.6\%}$	4.7	$0.17012(6)^{+8.6\%}_{-6.8\%}$	5.6	1.958	0.967
$Z_T W_L^+$	$0.08710(1)^{+0.1\%}_{-0.6\%}$	4.7	$0.24307(7)^{+10.2\%}_{-8.2\%}$	8.0	2.791	1.017
$Z_T W_T^+$	$0.97678(7)^{+2.0\%}_{-2.2\%}$	52.6	$2.0008(7)^{+8.9\%}_{-7.1\%}$	65.8	2.048	1.059
interf.	0.0595(1)	3.2	0.009(2)	0.4	–	–
unresolved, $Z(e^+e^-)W^+(J)$						
unpol.	$1.6879(2)^{+1.9\%}_{-2.1\%}$	100	$3.112(2)^{+7.6\%}_{-6.1\%}$	100	1.843	1.193
$Z_L W_L^+$	$0.61653(5)^{+1.0\%}_{-1.3\%}$	36.5	$0.6799(5)^{+0.9\%}_{-0.7\%}$	21.9	1.103	1.170
$Z_L W_T^+$	$0.06444(1)^{+0.7\%}_{-1.0\%}$	3.8	$0.17584(6)^{+10.8\%}_{-8.6\%}$	5.7	2.729	1.158
$Z_T W_L^+$	$0.07437(1)^{+0.6\%}_{-0.9\%}$	4.4	$0.24742(8)^{+11.0\%}_{-8.9\%}$	8.0	3.327	1.193
$Z_T W_T^+$	$0.88233(9)^{+2.9\%}_{-2.9\%}$	52.3	$2.0041(8)^{+9.6\%}_{-7.7\%}$	64.3	2.271	1.227
interf.	0.0503(3)	3.0	0.004(2)	0.1	–	–

- The interference contribution is small
- Interference becomes smaller at NLO

Comparison background

	resolved		unresolved	
process	σ_{LO} [fb]	ratio over full $O(\alpha^4)$	σ_{LO} [fb]	ratio over full $O(\alpha^4)$
DPA ZW^+	$1.8567(2)^{+1.2\%}_{-1.4\%}$	0.353	$1.6879(2)^{+1.9\%}_{-2.1\%}$	0.425
DPA ZW^-	$1.0527(1)^{+1.3\%}_{-1.6\%}$	0.200	$0.9003(1)^{+2.0\%}_{-2.1\%}$	0.227
DPA ZZ	$2.1430(3)^{+1.3\%}_{-1.6\%}$	0.408	$1.2804(2)^{+2.6\%}_{-2.7\%}$	0.323
DPA ZV	$5.0523(4)^{+1.3\%}_{-1.5\%}$	0.961	$3.8685(3)^{+2.2\%}_{-2.3\%}$	0.975
full $O(\alpha^4)$	$5.253(1)^{+1.2\%}_{-1.5\%}$	1.000	$3.967(2)^{+2.1\%}_{-2.3\%}$	1.000
full $O(\alpha_s\alpha^3)$	$-0.3124(6)^{+9.2\%}_{-10.7\%}$	-0.059	$-0.2145(6)^{+9.7\%}_{-11.4\%}$	-0.054
full $O(\alpha_s^2\alpha^2)$	$97.91(7)^{+24.3\%}_{-18.4\%}$	18.638	$62.55(7)^{+25.0\%}_{-18.8\%}$	15.768

- Non-resonant background
- Resonant ZZ and ZW^- pair production background
  - Have to be treated as additional contributions

Comparison background

	resolved		unresolved	
process	σ_{LO} [fb]	ratio over full $O(\alpha^4)$	σ_{LO} [fb]	ratio over full $O(\alpha^4)$
DPA ZW^+	$1.8567(2)^{+1.2\%}_{-1.4\%}$	0.353	$1.6879(2)^{+1.9\%}_{-2.1\%}$	0.425
DPA ZW^-	$1.0527(1)^{+1.3\%}_{-1.6\%}$	0.200	$0.9003(1)^{+2.0\%}_{-2.1\%}$	0.227
DPA ZZ	$2.1430(3)^{+1.3\%}_{-1.6\%}$	0.408	$1.2804(2)^{+2.6\%}_{-2.7\%}$	0.323
DPA ZV	$5.0523(4)^{+1.3\%}_{-1.5\%}$	0.961	$3.8685(3)^{+2.2\%}_{-2.3\%}$	0.975
full $O(\alpha^4)$	$5.253(1)^{+1.2\%}_{-1.5\%}$	1.000	$3.967(2)^{+2.1\%}_{-2.3\%}$	1.000
full $O(\alpha_s\alpha^3)$	$-0.3124(6)^{+9.2\%}_{-10.7\%}$	-0.059	$-0.2145(6)^{+9.7\%}_{-11.4\%}$	-0.054
full $O(\alpha_s^2\alpha^2)$	$97.91(7)^{+24.3\%}_{-18.4\%}$	18.638	$62.55(7)^{+25.0\%}_{-18.8\%}$	15.768

- DPA approximates the full electroweak process well (2% – 4%)

Comparison background

	resolved		unresolved	
process	σ_{LO} [fb]	ratio over full $O(\alpha^4)$	σ_{LO} [fb]	ratio over full $O(\alpha^4)$
DPA ZW^+	$1.8567(2)^{+1.2\%}_{-1.4\%}$	0.353	$1.6879(2)^{+1.9\%}_{-2.1\%}$	0.425
DPA ZW^-	$1.0527(1)^{+1.3\%}_{-1.6\%}$	0.200	$0.9003(1)^{+2.0\%}_{-2.1\%}$	0.227
DPA ZZ	$2.1430(3)^{+1.3\%}_{-1.6\%}$	0.408	$1.2804(2)^{+2.6\%}_{-2.7\%}$	0.323
DPA ZV	$5.0523(4)^{+1.3\%}_{-1.5\%}$	0.961	$3.8685(3)^{+2.2\%}_{-2.3\%}$	0.975
full $O(\alpha^4)$	$5.253(1)^{+1.2\%}_{-1.5\%}$	1.000	$3.967(2)^{+2.1\%}_{-2.3\%}$	1.000
full $O(\alpha_s\alpha^3)$	$-0.3124(6)^{+9.2\%}_{-10.7\%}$	-0.059	$-0.2145(6)^{+9.7\%}_{-11.4\%}$	-0.054
full $O(\alpha_s^2\alpha^2)$	$97.91(7)^{+24.3\%}_{-18.4\%}$	18.638	$62.55(7)^{+25.0\%}_{-18.8\%}$	15.768

- Very large QCD background that needs to be subtracted before carrying out a polarisation analysis

Differential results

- Differential cross-sections show the dependence on physical observables
- Differences of the two setups and the polarisation states
- Polarisation dependent variables are of particular interest
- Shapes of the distributions are needed for the measurement of polarisation fractions

Electron decay angle $\cos\left(\vartheta^{*,\mathrm{CM}}_{e^-}\right) = \dfrac{\vec{p}^{\,*}_{e^-} \cdot \vec{p}^{\,\mathrm{CM}}_{e^+e^-}}{|\vec{p}^{\,*}_{e^-}|\,|\vec{p}^{\,\mathrm{CM}}_{e^+e^-}|}$

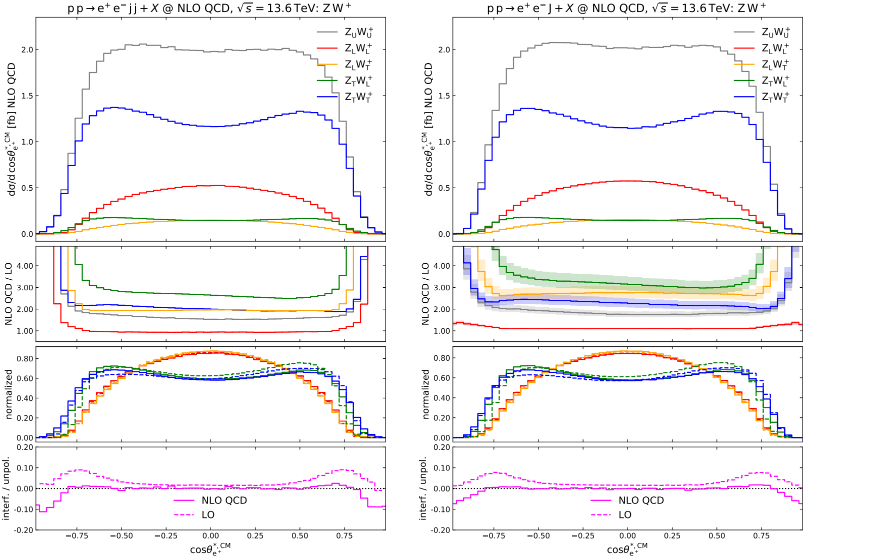

Electron decay angle $\cos\left(\vartheta^{*,\mathrm{CM}}_{e^-}\right) = \frac{\vec{p}^{\,*}_{e^-} \cdot \vec{p}^{\,\mathrm{CM}}_{e^+e^-}}{|\vec{p}^{\,*}_{e^-}||\vec{p}^{\,\mathrm{CM}}_{e^+e^-}|}$

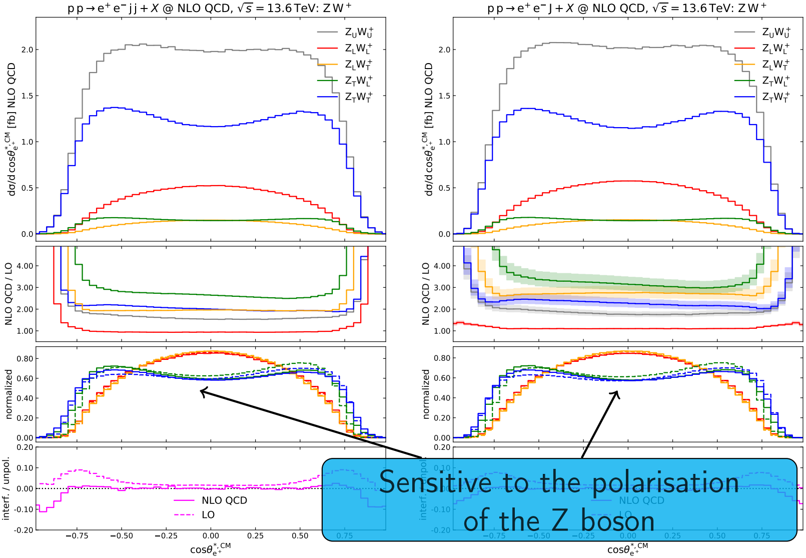

Sensitive to the polarisation of the Z boson

Electron decay angle $\cos\left(\vartheta^{*,\mathrm{CM}}_{e^-}\right) = \frac{\vec{p}^{\,*}_{e^-} \cdot \vec{p}^{\,\mathrm{CM}}_{e^+e^-}}{|\vec{p}^{\,*}_{e^-}||\vec{p}^{\,\mathrm{CM}}_{e^+e^-}|}$

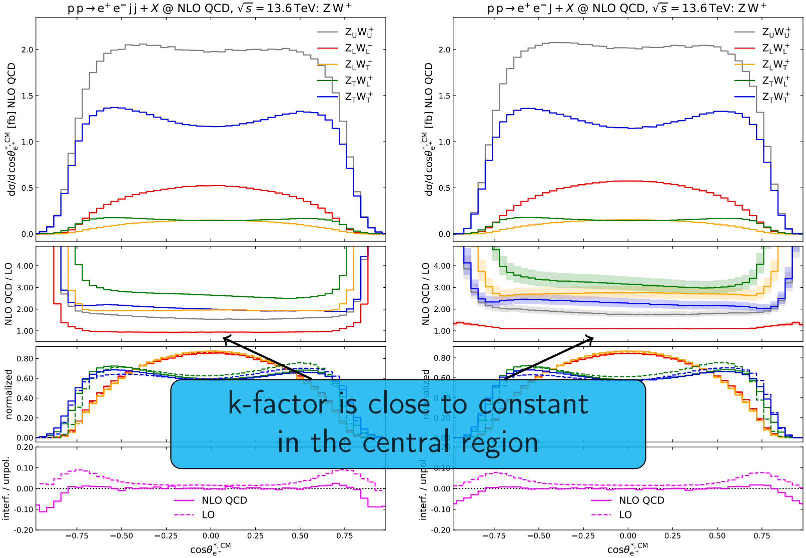

Positron transverse momentum $p_{T,e^+} = \sqrt{p_{1,e^+}^2 + p_{2,e^+}^2}$

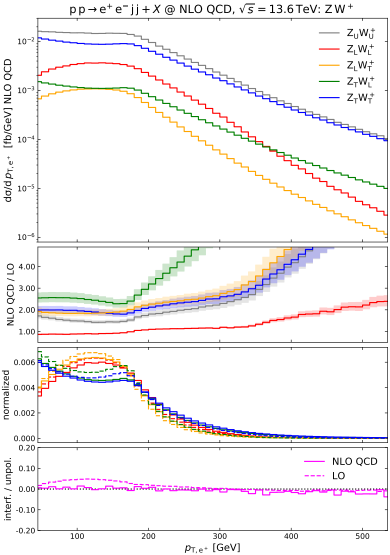

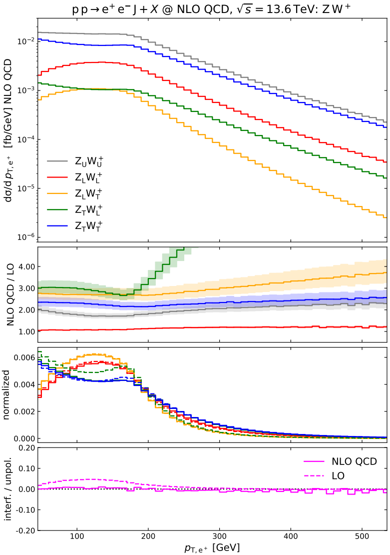

Positron transverse momentum $p_{T,e^+} = \sqrt{p^2_{1,e^+} + p^2_{2,e^+}}$

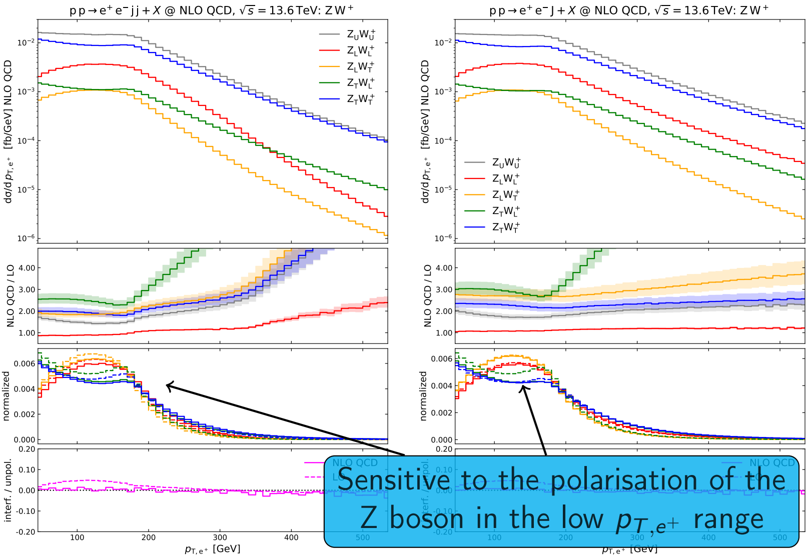

Sensitive to the polarisation of the Z boson in the low p_{T,e^+} range

Positron transverse momentum $p_{T,e^+} = \sqrt{p_{1,e^+}^2 + p_{2,e^+}^2}$

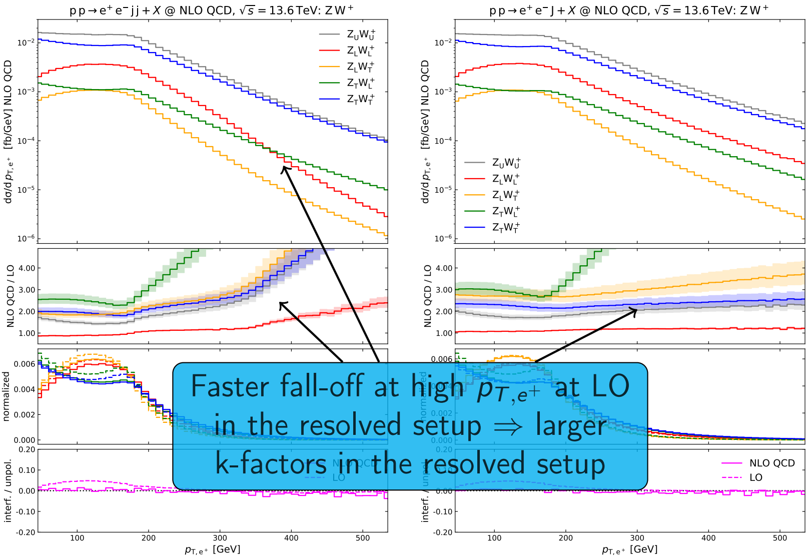

Scattering angle $\cos(\vartheta_{scatt}) = \frac{|p^{\mathrm{CM}}_{e^+e^-,z}|}{|\vec{p}^{\,\mathrm{CM}}_{e^+e^-}|}$

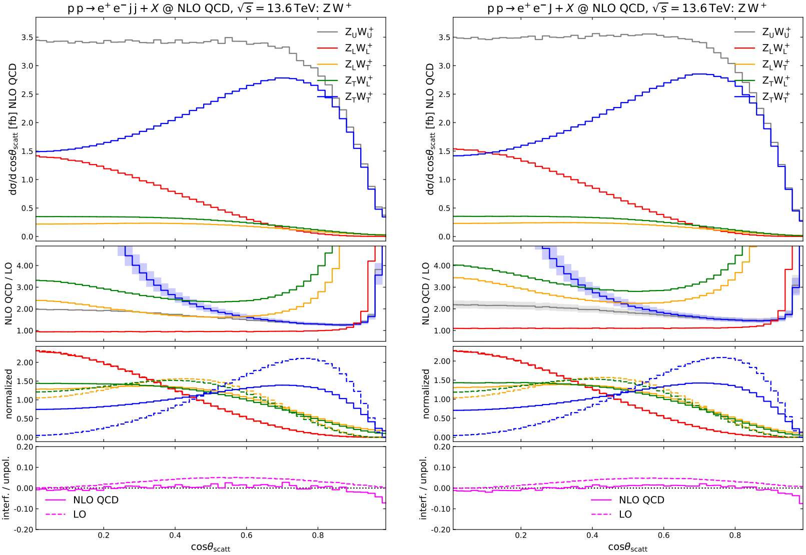

Scattering angle $\cos(\vartheta_{scatt}) = \frac{|p^{\rm CM}_{e^+e^-,z}|}{|\vec{p}^{\rm CM}_{e^+e^-}|}$

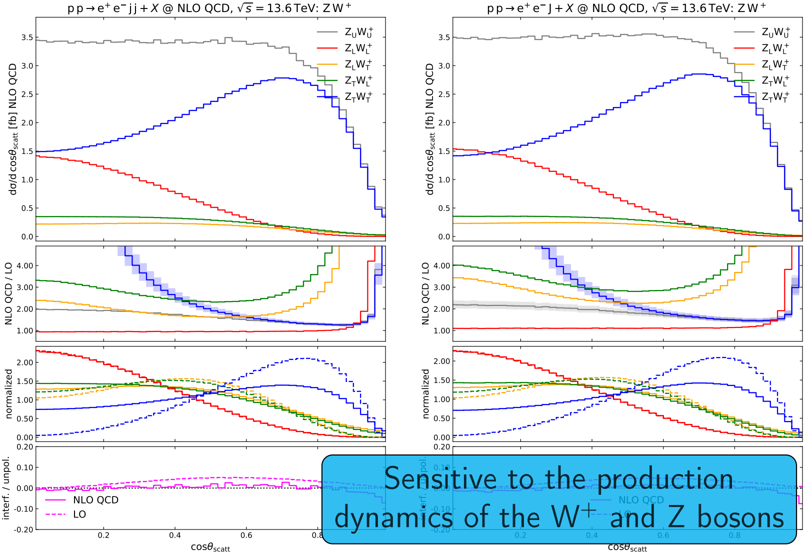

Sensitive to the production dynamics of the W^+ and Z bosons

Scattering angle $\cos(\vartheta_{scatt}) = \frac{|p^{\rm CM}_{e^+e^-,z}|}{|\vec{p}^{\,\rm CM}_{e^+e^-}|}$

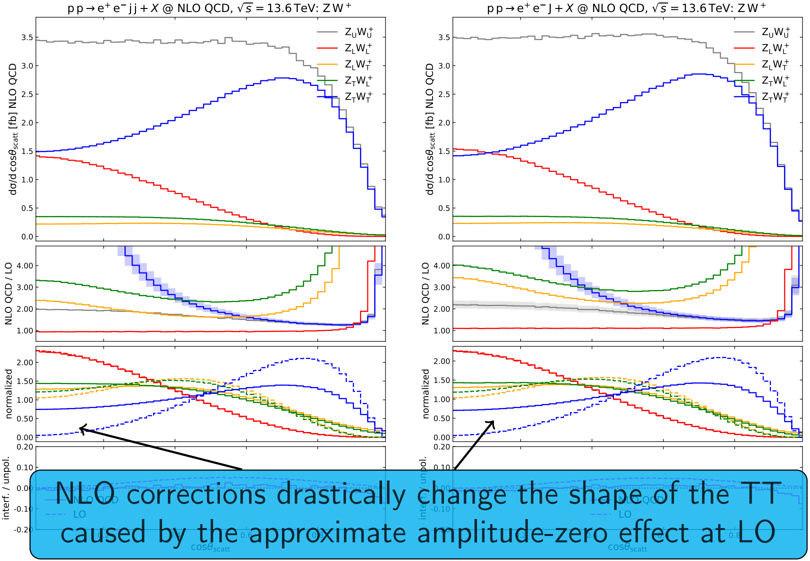

NLO corrections drastically change the shape of the TT caused by the approximate amplitude-zero effect at LO

Invariant mass jet-system $M_J = \sqrt{p_J^2}$

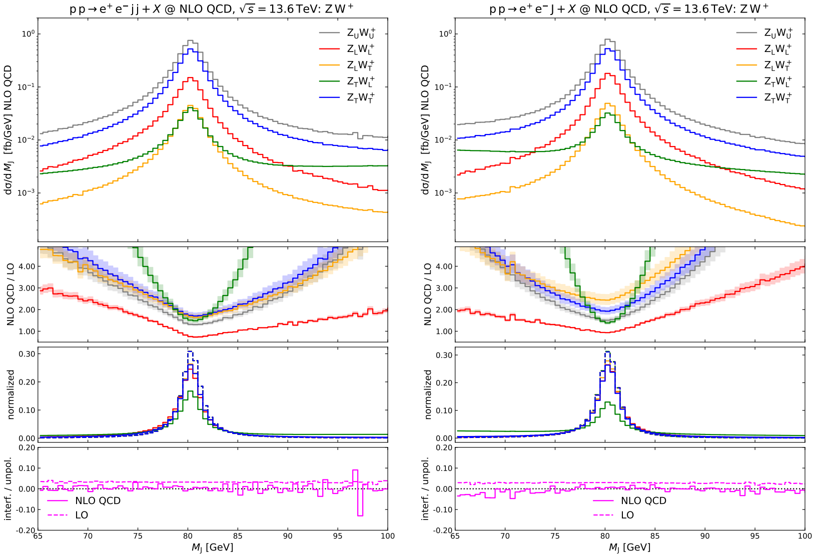

Invariant mass jet-system $M_J = \sqrt{p_J^2}$

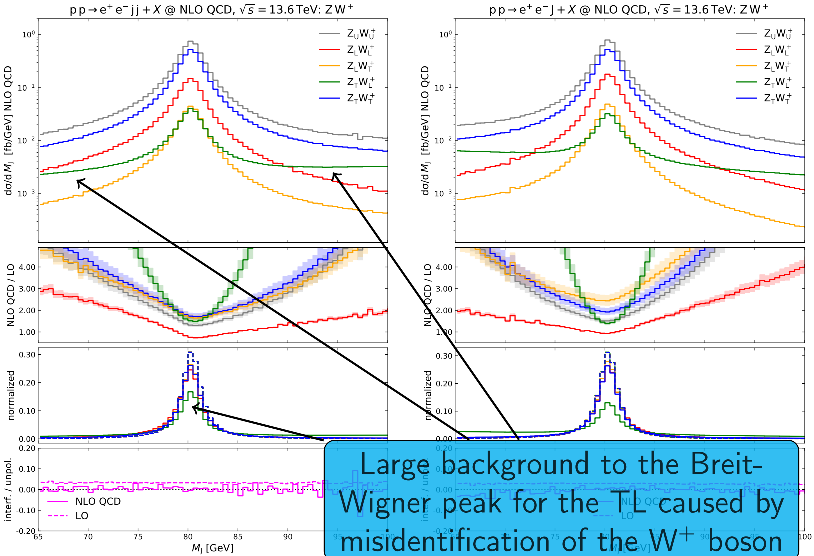

Large background to the Breit-Wigner peak for the TL caused by misidentification of the W^+ boson

Decay angle hardest decay-jet $\cos\left(\vartheta^{*,\mathrm{CM}}_{j_1}\right) = \frac{\vec{p}^{\,*}_{j_1} \cdot \vec{p}^{\,\mathrm{CM}}_{\mathrm{J}}}{|\vec{p}^{\,*}_{j_1}||\vec{p}^{\,\mathrm{CM}}_{\mathrm{J}}|}$

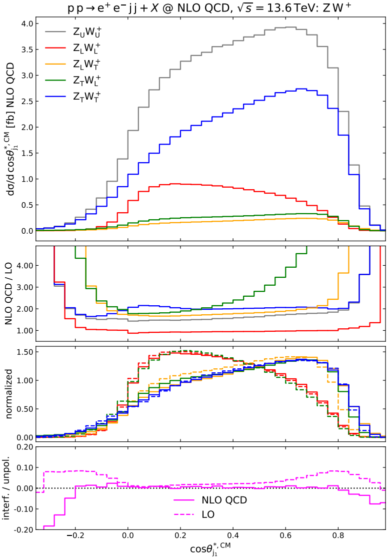

Decay angle hardest decay-jet $\cos\left(\vartheta_{j_1}^{*,\mathrm{CM}}\right) = \frac{\vec{p}_{j_1}^{\,*} \cdot \vec{p}_{\mathrm{J}}^{\,\mathrm{CM}}}{|\vec{p}_{j_1}^{\,*}||\vec{p}_{\mathrm{J}}^{\,\mathrm{CM}}|}$

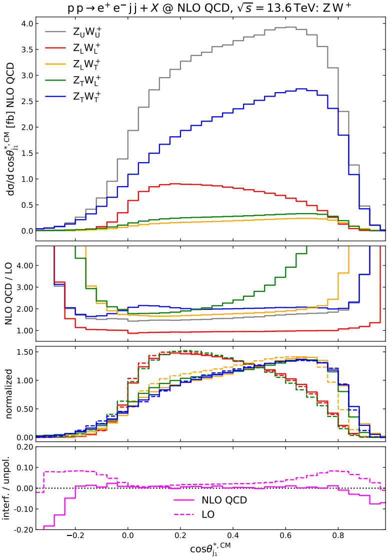

This variable is very sensitive to the polarisation of the W^+ boson similar to the decay angles of the leptons

The jets can only be distinguished by their transverse momentum or other measurable quantities not by their flavour

Decay angle hardest decay-jet $\cos\left(\vartheta^{*,\mathrm{CM}}_{j_1}\right) = \frac{\vec{p}^{\,*}_{j_1} \cdot \vec{p}^{\,\mathrm{CM}}_{\mathrm{J}}}{|\vec{p}^{\,*}_{j_1}||\vec{p}^{\,\mathrm{CM}}_{\mathrm{J}}|}$

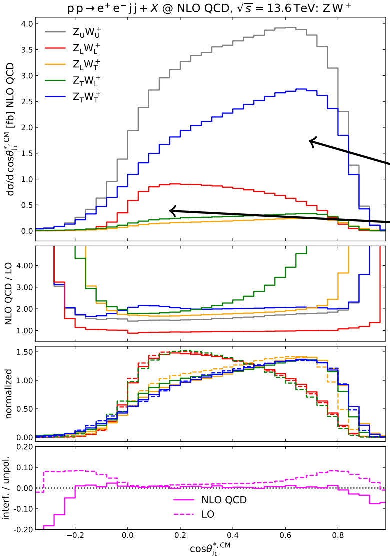

Hardest jet is predominantly emitted in the direction of the jet system

Decay angle hardest decay-jet $\cos\left(\vartheta^{*,\mathrm{CM}}_{j_1}\right) = \frac{\vec{p}^{*}_{j_1} \cdot \vec{p}^{\,\mathrm{CM}}_{\mathrm{J}}}{|\vec{p}^{*}_{j_1}||\vec{p}^{\,\mathrm{CM}}_{\mathrm{J}}|}$

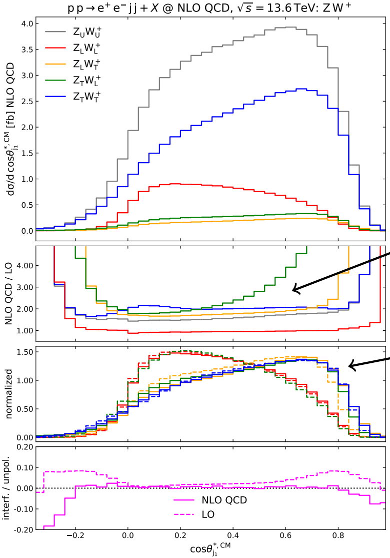

k-factor is flat in the central region for LL, TT, LT

TL has a large shape change from LO to NLO

Summary

- Calculated the polarised cross-sections for ZW^+ production with semileptonic decay
  - Used the double-pole approximation to define polarised ZW^+ production
  - Used methods can be directly extended to the calculation of the NLO QCD corrections to semileptonic decays of other processes
    - Resonant background ZZ and ZW^- production
    - Vector-boson pair production processes
    - Vector-boson scattering processes
- Hadronic decays are different from purely leptonic decays
  - Higher event rate
  - Very large QCD background and resonant ZZ, ZW^- background
- Many observables are well suited to distinguish the polarisation states
  - This sensitivity remains even when the jets are recombined to one jet and become indistinguishable (unresolved setup)

Bibliography I

- D. Buarque Franzosi, O. Mattelaer, R. Ruiz, and S. Shil, *Automated predictions from polarized matrix elements*, *JHEP* **04** (2020) 082, [arXiv:1912.01725].
- A. Denner and G. Pelliccioli, *NLO QCD predictions for doubly-polarized WZ production at the LHC*, *Phys. Lett. B* **814** (2021) 136107, [arXiv:2010.07149].
- D. N. Le and J. Baglio, *Doubly-polarized WZ hadronic cross sections at NLO QCD+EW accuracy*, arXiv:2203.01470.
- D. N. Le, J. Baglio, and T. N. Dao, *Doubly-polarized WZ hadronic production at NLO QCD+EW: Calculation method and further results*, arXiv:2208.09232.
- T. N. Dao and D. N. Le, *Enhancing the doubly-longitudinal polarization in WZ production at the LHC*, arXiv:2302.03324.

Bibliography II

- ATLAS Collaboration, *Measurement of $W^{\pm}Z$ production cross sections and gauge boson polarisation in pp collisions at $\sqrt{s} = 13$ TeV with the ATLAS detector*, *Eur. Phys. J. C* **79** (2019) 535, [arXiv:1902.05759].
- CMS Collaboration, *Measurement of the inclusive and differential WZ production cross sections, polarization angles, and triple gauge couplings in pp collisions at $\sqrt{s} = 13$ TeV*, *Journal of High Energy Physics* **2022** (jul, 2022) [arXiv:2110.11231].
- ATLAS Collaboration, *Observation of gauge boson joint-polarisation states in $W^{\pm}Z$ production from pp collisions at $\sqrt{s} = 13$ TeV with the ATLAS detector*, arXiv:2211.09435.

Bibliography III

CMS Collaboration, *Search for heavy resonances decaying to ZZ or ZW and axion-like particles mediating nonresonant ZZ or ZH production at $\sqrt{s}$ =13 TeV*, *JHEP* **04** (2022) 087, [arXiv:2111.13669].

Backup Slides

Dominant Diagrams LT TL

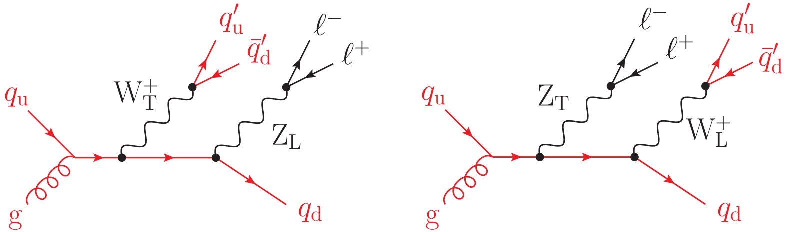

- For these diagrams the longitudinally polarised boson and the additional quark are predominantly emitted in a similar spatial direction
- This allows for a lower transverse momentum of the longitudinally polarised boson
- The lower transverse momentum leads to less unitarity cancellations

Results without p_T cut on the jet system

state	σ_{LO} [fb]	f_{LO}[%]	σ_{NLO} [fb]	f_{NLO}[%]	K_{NLO}	$K_{\mathrm{NLO}}^{(\mathrm{no\ g})}$
resolved (no minimum *ptjj* cut), $Z(e^+e^-)W^+(jj)$						
unpol.	$1.8564(1)^{+1.2\%}_{-1.4\%}$	100	$5.5388(8)^{+10.6\%}_{-8.6\%}$	100	2.984	1.371
$Z_L W_L^+$	$0.64605(3)^{+0.2\%}_{-0.6\%}$	34.8	$0.7525(4)^{+1.5\%}_{-1.2\%}$	13.6	1.165	1.194
$Z_L W_T^+$	$0.08687(1)^{+0.2\%}_{-0.6\%}$	4.7	$0.3057(1)^{+11.4\%}_{-9.2\%}$	5.5	3.519	1.462
$Z_T W_L^+$	$0.08710(1)^{+0.1\%}_{-0.6\%}$	4.7	$1.0486(1)^{+14.6\%}_{-11.9\%}$	18.9	12.04	2.408
$Z_T W_T^+$	$0.97677(7)^{+2.0\%}_{-2.2\%}$	52.6	$3.5506(9)^{+11.8\%}_{-9.6\%}$	64.1	3.635	1.424
interf.	0.0595(1)	3.2	−0.119(2)	−2.1	–	–

- LO results are unchanged
- NLO corrections become larger in particular for TL

Results without p_T cut on the jet system

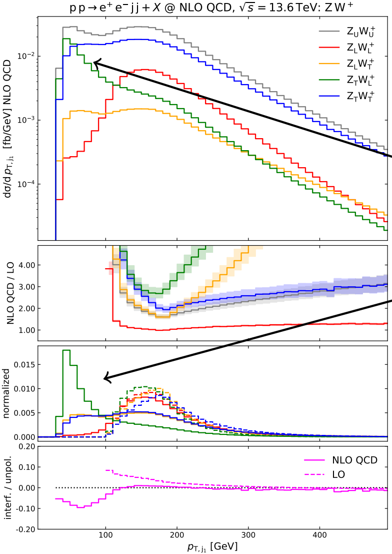

Large peak in the low p_{T,j_1} region of TL is cut away by transverse momentum cut on the W^+ boson

Results without p_T cut on the jet system

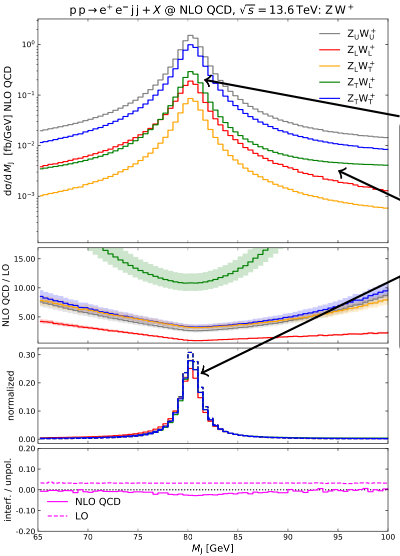

Breit-Wigner peak is now unsupressed

Background still exists but is smaller compared to the peak